Della Pietra, M.; Discepoli, G.; Bosio, B.; Mcphail, S.; Barelli, L.; Bidini, G.; Ribes-Greus, A. (2016). Experimental investigation of SO2 poisoning in a Molten Carbonate Fuel Cell operating in CCS configuration. International Journal of Hydrogen Energy. 41(41):18822-18836. https://doi.org/10.1016/j.ijhydene.2016.05.147

Experimental investigation of SO_2 poisoning in a Molten Carbonate Fuel Cell operating in CCS configuration

Massimiliano Della Pietra[a,b], Gabriele Discepoli[b], Barbara Bosio[c], Stephen J. McPhail[a], Linda Barelli[b],Gianni Bidini[b], Ribes-Greus Amparo[d]

[a]ENEA R.C. Casaccia,
Technical Unit Renewable Sources,
Via Anguillarese 301, 00123 Rome, Italy

[b]Department of Engineering,
University of Perugia,
via G. Duranti 67 ,06100 Perugia, Italy

[c]PERT, DICCA,
University of Genova,
Via Opera Pia 15, 16145 Genova, Italy

[d]Instituto de Tecnología de Materiales,
Universidad Politecnica de Valencia,
Camino de Vera s/n, 46022, Sivilla,Spain

Corresponding author max.dellapietra@gmail.com

Experimental investigation of SO_2 poisoning in a Molten Carbonate Fuel Cell operating in CCS configuration

Massimiliano Della Pietra[a,b], Gabriele Discepoli[b], Barbara Bosio[c], Stephen J. McPhail[a], Linda Barelli[b],Gianni Bidini[b], Ribes-Greus Amparo[d]

Abstract

One of the most interesting innovations in the CCS (Carbon Capture and Storage) field is the use of MCFCs as carbon dioxide concentrators, feeding their cathode side (or air side) with the exhaust gas of a traditional power plant. The feasibility of this kind of application depends on the resistance of the MCFC to air-side contaminants, with particular attention to SO_2. The aim of this work is to investigate the effects of poisoning when sulphur dioxide is added to the cathodic stream in various concentrations and in different operating conditions. This study was carried out operating single cells (80 cm^2) with a cathodic feeding composition simulating typical flue gas conditions, i.e. N_2, H_2O, O_2 and CO_2 in 73:9:12:6 mole ratio as reference mixture. On the anodic side a base composition was chosen with H_2, CO_2 and H_2O in 64:16:20 mole ratio. Starting from these reference mixtures, the effect of single species on cell poisoning was experimentally investigated considering, as main parameters chosen for the sensitivity analysis, SO_2 (0-24ppm) and CO_2 (4-12%) content in the cathodic feeding mixture, H_2 (40-64%) content in the anodic stream as well as the operating temperature (620-680°C). Results showed that degradation caused by SO_2 poisoning is strongly affected by the operating conditions. Data gathered during this experimental campaign will be used in a future work to model the poisoning mechanisms through the definition of MCFC electrochemical kinetics which take into account the SO_2 effects.

Keywords

MCFC, CCS, sulphur poisoning, sensitivity analysis

1. Introduction

Recently the public awareness concerning greenhouse gases emissions, with particular reference to CO_2, has significantly increased.

It seems clear that the problem of global warming caused by greenhouse gases has to be tackled using a plurality of solutions and technologies to obtain results in short, medium and long term periods. In this scenario Carbon Capture and Storage (CCS) appears to be a suitable "bridge" technology in the transition to a low carbon economy. CCS, in fact, contributes to reducing atmospheric emissions coming from fossil fuel power plants, giving the needed time to renewable sources to reach an appropriate technology readiness level, in order to be a profitable alternative from economical and technical point of view.

Thanks to the reactions occurring at anode and cathode (reactions 1, 2), the MCFC can be considered a CO_2 concentrator. It transfers diluted CO_2 present at the cathode side to the anode side, where it is highly concentrated in a stream composed of just CO_2, H_2O and a small amount of unreacted fuel; thus CO_2 is easily separable from the anodic outlet.

$$(1)\ H_2 + CO_3^{2-} \rightarrow H_2O + CO_2$$

$$(2)\ CO_2 + \frac{1}{2}O_2 + 2e^- \rightarrow CO_3^{2-}$$

The MCFC thus behaves as an *active* CCS technology, *producing* electric power (instead of consuming it in the case of passive technologies as ammine scrubbing) while removing carbon dioxide from the exhaust gases of traditional power plants.

Such post-combustion carbon dioxide separation is most effective applied to coal combustion and combined cycle power generation, due to the large potential of CO_2 reduction from these plants. The flue gas from these types of combustion technologies typically contains 3-12% CO_2 and residual O_2, both in the lower operational range of the MCFC: the stability of operation in these conditions has been studied experimentally in [1–8]. Several other studies have assessed the integration of an MCFC as CCS retrofit approaching the topic with numerical models, considering the same ranges of CO_2 content [9–13].

However, the greatest barrier to the feasibility of this application is the presence of pollutants in the flue gas entering the cathode. In CCS, SO_2 is the most harmful pollutant agent present in the flue gas, which causes performance decay and structural degradation of the MCFC. It is known that SO_2 content can significantly affect the cell performance as discussed in previous works [14–16]. Specifically, in [14] long term tests allowed to investigate the evolution of the sulphur poisoning mechanism under fixed operating conditions and concentrations of the pollutant agent. To provide a complete framework, necessary to perform quantitative analysis of this phenomenon, investigation must be carried out to characterize the effect of the main operating parameters on SO_2 poisoning. The objective of the present work addresses extended and immediate sulphur dioxide poisoning effects and how these are affected by the variation of operating parameters as SO_2 (0-24ppm) and CO_2 (4-12%) contents in the cathodic feeding mixture, H_2 (40-64%) content in the anodic stream, as well as the operating temperature (620-680 °C). All the obtained data of this in-depth sensitivity analysis will be used in a future work to validate a kinetic model of the MCFC which takes into account also the poisoning due to SO_2.

2. SO_2 effects

There are few literature contributions concerning the interactions between SO_2 and MCFC, since this poisoning mechanism has not been studied as intensely as that of other pollutants like H_2S. Consequently, it is not easy to predict the effects of sulphur dioxide during the life of a cell. It appears that reactions, occurring when SO_2 is fed to the cathode, involve directly the electrolyte.

$$(3)\ CO_3^{2-} + SO_2 + \frac{1}{2}O_2 \rightarrow SO_4^{2-} + CO_2$$

$$(4)\ H_2S + CO_3^{2-} + 3H_2O \leftrightarrow SO_4^{2-} + CO_2 + 4H_2$$

Specifically, SO_2 is converted to sulphate by reaction (3); consequently, under load, sulphate ions migrate to the anode, accumulating in the electrolyte. At the anode side sulphur is released as H_2S according to the reverse of reaction (4).

Beyond corrosion of metallic parts, sulphur causes poisoning both due to loss of CO_3^{2-} charge carriers in the electrolyte (3), as due to H_2S released from the electrolyte at the anode side.

The effects of hydrogen sulphide on MCFC components have been deeply investigated [17–23]. In particular, H_2S reacts:

- according with chemisorption (5) and adsorption (6) reactions [20], on the anode nickel surface

$$(5)\ Ni_{(s)} + H_2S_{(g)} \rightarrow Ni - H_2S_{(ads)}$$

$$(6)\ Ni_{(s)} + H_2S_{(g)} \rightarrow Ni - HS_{(ads)} + Ni - H_{(ads)} \rightarrow Ni - S_{(ads)} + Ni + H_{2(g)}$$

- chemically (7)-(8) [17]

$$(7)\ Ni + H_2S \rightarrow NiS + H_2$$

$$(8)\ 3Ni + xH_2S \rightarrow Ni_3S_X + xH_2$$

- electrochemically (9)-(10) [17]

$$(9)\ Ni + S^{2-} \rightarrow NiS + 2e^-$$

$$(10)\ 3Ni + xS^{2-} \rightarrow Ni_3S_X + 2xe^-$$

The effects of these reactions depend on chemical and electrochemical conditions, but all contribute to decreasing cell performance, forming nickel sulphides on the anode surface. The latter block active sites meant for hydrogen oxidation, covering the pore network and changing the wettability of the electrolyte.

3. Experimental method

In operando analysis, polarisation curves and electrochemical impedance spectroscopy (EIS), was performed at two different laboratories (ENEA hotlab, UNIPG fuel cell laboratory) on state-of-the-art single cells (active area 80 cm^2). The experimental campaign was structured to simulate CCS conditions: in the large cathodic compared to the anodic flow rate, in the CO_2 content in the cathodic stream as well as in its humidification.

According to the main objective of the study, operating conditions, in terms of cell temperature and both cathodic (SO_2 and CO_2) and anodic (H_2) compositions, were suitably varied to comprehend a significant and consistent range of working points. The variation of anodic and cathodic reactants was inspired by a previous work [24] performed in clean condition without any addition of pollutant agents.

The poisoning protocol was structured in order to recognize the transfer mechanism of sulphur from cathode side to anode side and, at the same time, to study the accumulation of sulphur ions in the electrolyte.

Table 1 summarizes the considered parameters and the corresponding variation range. Specifically, boldface values correspond to the “Standard” conditions, tested also in absence of SO_2 for

benchmarking, while the other values refer to all working points systematically taken into account for the sensitivity analysis.

Four different concentrations of SO_2 (4/8/16/24 ppm) were tested. For each SO_2 concentration, the other operating parameters (hydrogen and cathodic carbon dioxide) were varied, maintaining constant anodic and cathodic flow rates. To this aim nitrogen was used to compensate the variation of H_2 and CO_2.

Anode side	**Molar fraction (%)**	**Flow rate (Sccm/cm^2)**
H_2	**64**/52/40 %	1.67/1.36/1.04
CO_2	**16%**	0.42
H_2O	**20%**	0.52
N_2	**0**/12/24%	0/0.31/0.63
TOT		2.61
Cathode side	**Molar fraction (%)**	**Flow rate (Sccm/cm^2)**
N_2	**73**/75/67%	18.32/18.82/16.81
O_2	**12%**	2.75
CO_2	**6**/4/12%	1.5/1/3.01
H_2O	**9%**	2.26
TOT		25.09
Cell Temp.	**650**/620/680°C	-
SO_2at the cathode	**0 ("clean")/4/8/16/24 ppm**	-

Table 1: Operating parameters for the experimental campaign

Finally, the whole test campaign (initially performed at 650°C) was repeated at 620°C and 680°C working temperature. Globally, for each relevant parameter (H_2, CO_2, and operating temperature) four different SO_2 contents (4/8/16/24 ppm) as well as a "clean" benchmark were considered, leading to a test matrix of over 40 different analysed conditions.

As already mentioned before the experimental campaign was carried out in two different testing laboratories (ENEA hotlab and fuel cell laboratory at University of Perugia); table 2 summarizes cell specimens used for the experimentation with the indication of the testing laboratory.

Poisoning tested conditions	**Cells**	**Testing laboratory**
Clean	single cell #1	ENEA
Low content of SO_2 4 ppm		
Medium content of SO_2 8 ppm	single cell #2	ENEA
High content of SO_2 24 ppm		
Medium/high content of SO_2 16 ppm	single cell #3	University of Perugia

Table 2: single cells and test benches used.

As already mentioned before, the interactions between sulphur dioxide and cell components are various and of different nature. Because of this, measurements of MCFC performance were initiated only after H_2S was observed and stabilized at the anode outlet, thereby assuming that the reverse of reaction (4), as all other poisoning mechanisms, had achieved equilibrium conditions. The quantification of the amount of H_2S at the anode was performed, using colorimetric syringe (prod: Kitagawa; mod: 120SE).

The experimental campaign, described above, was carried out aiming to characterize the effect of

operating parameters on the degradation mechanism. Figure 1 summarizes how the experimental campaign was conducted.

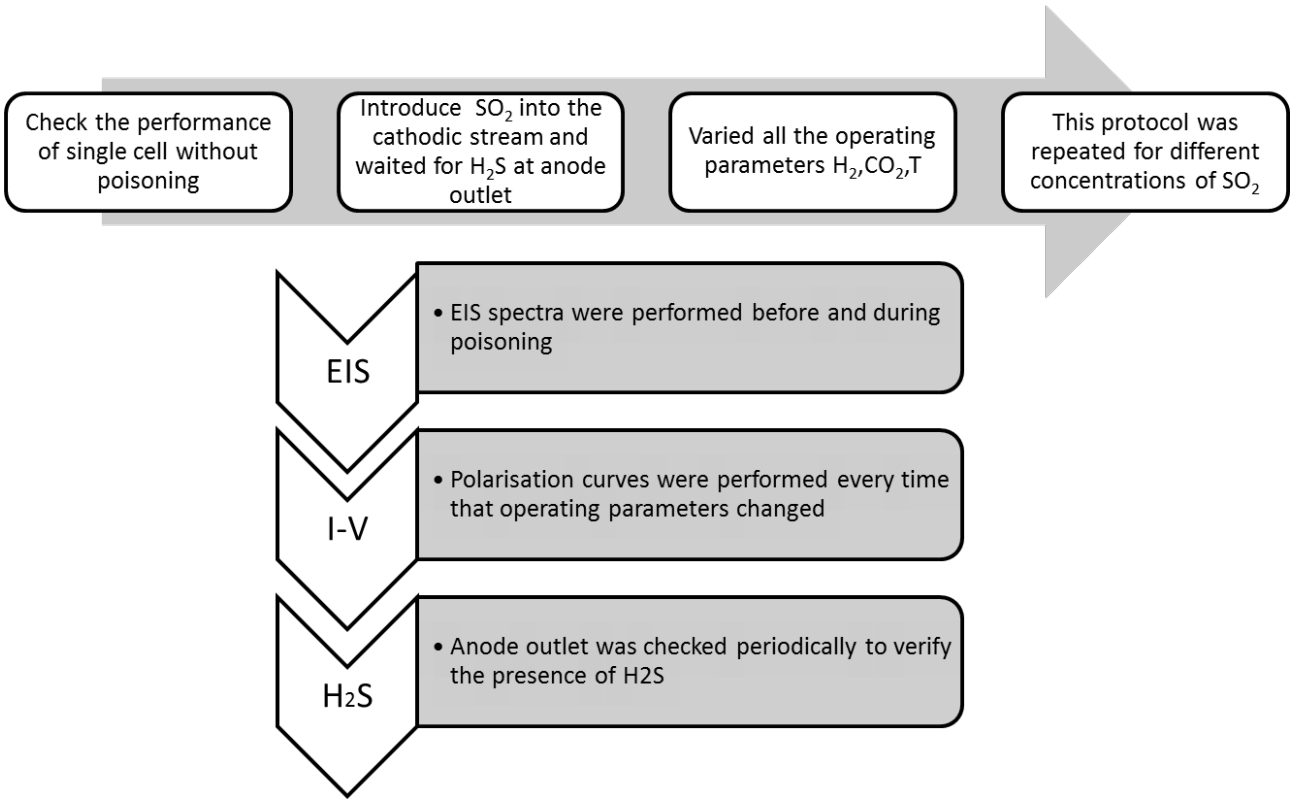

Figure 1: schematic representation of experimental campaign: horizontal arrow showing the logic of the variation of the parameters, vertical arrow shows the sequence of the "in operando" analysis conducted for each step of the experimental campaign.

To better understand the occurred degradation phenomena, also post mortem analysis was carried out. Specifically, EDX analysis was performed after test exposure under medium/high poisoning conditions. Moreover, to complete the experimental characterization of the SO_2 effects on the operating MCFC, a long-term test was carried out under 1 ppm SO_2 in Standard conditions (see Table 1), as opposed the sensitivity measurements carried out at higher concentrations and shorter durations. This test, performed on a further virgin cell (specimen #4), was specifically targeted to obtain representative results in post-test analysis.

4. Results and discussion

Kinetic characterization of poisoning mechanisms

The first set of experiments were performed on cell #1 in “clean” conditions, varying operating parameters (excluding temperature) without any addition of sulphur dioxide; this was necessary to have a strong reference for the future comparison of the “polluted” results.

Experiments under clean conditions, plotted as polarisation curves in fig. 2, are sensitive to the variation of cathodic CO_2 and anodic H_2. A systematic increase in cell voltage can be observed with increasing reagent concentration, where the cathodic CO_2 emerges as the crucial parameter for the cell performance. In the region of high current densities representative of mass transport phenomena, this behaviour is confirmed by the EIS spectra (fig. 3), which show an increase of the low-frequency semicircle when the CO_2 concentration decrease.

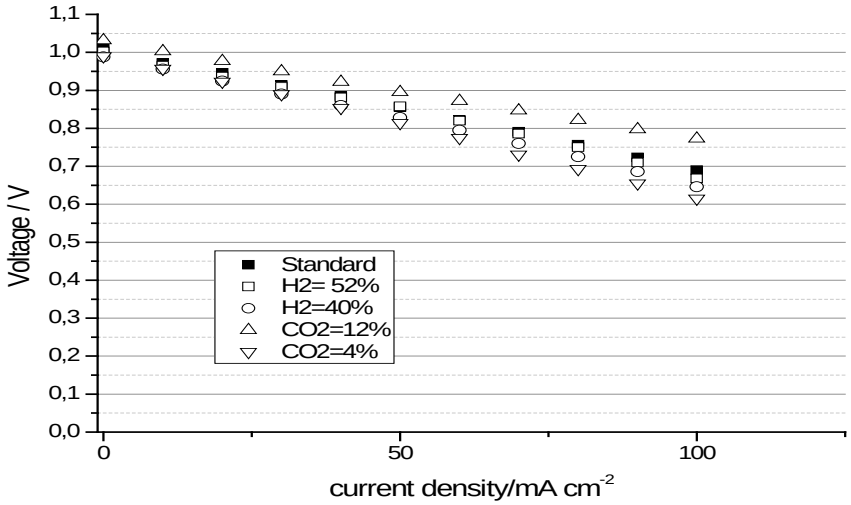

Figure 2: Polarisation curves using clean gas @650 °C (Standard composition: H_2= 64% ; CO_2= 6%). Polarisation curves in clean conditions show a significant dependence on the CO_2 concentration in the cathodic stream.

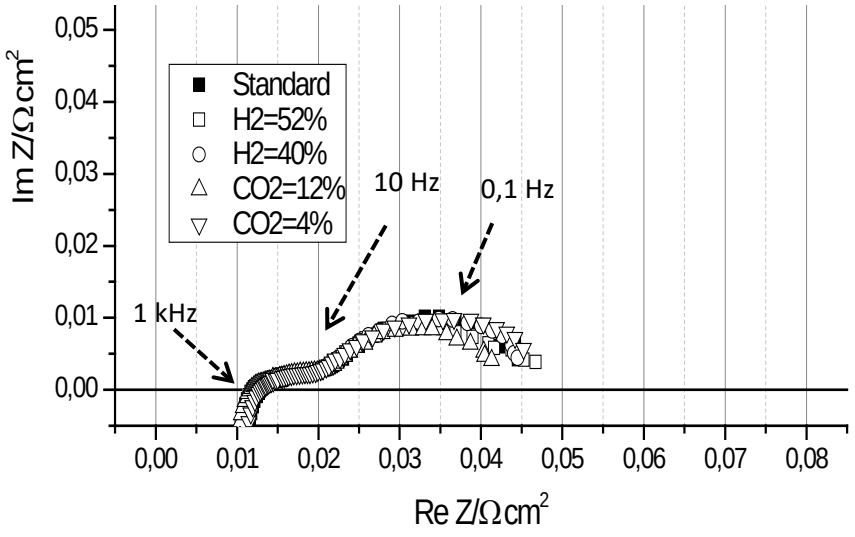

Figure 3: EIS spectra using clean gas @650 °C (Standard composition: H_2= 64% ; CO_2= 6%). EIS spectra confirm what found with the polarisation curves showing a lower mass transfer resistance for higher concentrations of cathodic CO_2.

After the tests under clean conditions, 4 ppm of sulphur dioxide were introduced in the cathodic stream. After 36 hours a small amount of H_2S (< 1ppm) was detected at the anodic outlet, confirming that SO_4^{2-} ions were reacting with the H_2 fed to the anode forming H_2S (following the reverse of reaction 4). Compared to the EIS spectrum in clean conditions (at 650 °C, fig. 3), although H_2S was revealed at the anode outlet (case of 4 ppm SO_2 fed at the cathode) indicating sulphur transfer through the cell, no appreciable change in EIS spectra can be detected (fig. 4a). Figures 4 a, b and c show the response of the poisoned cell #1 at the 3 different investigated temperatures.

a)

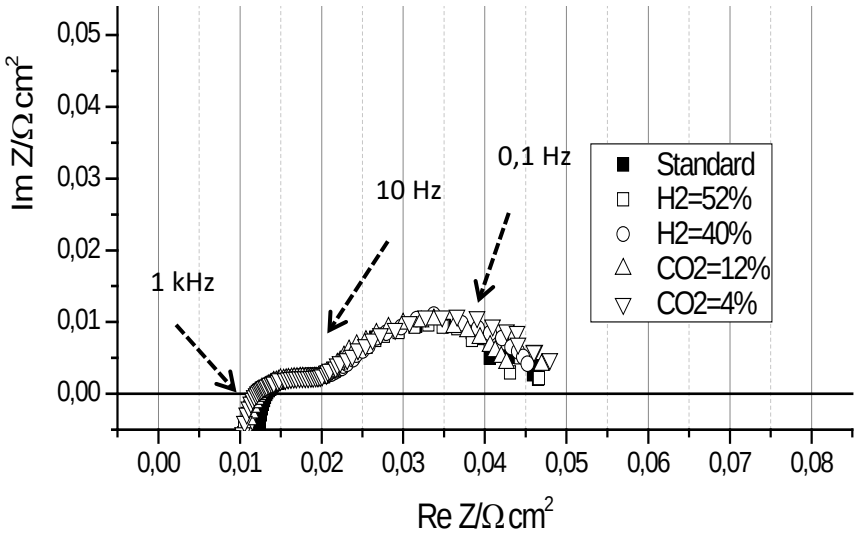

b)

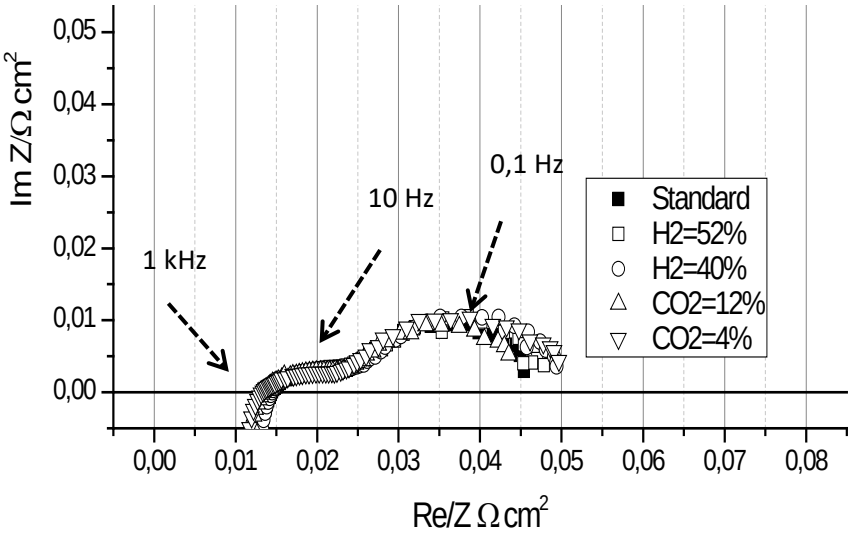

c)

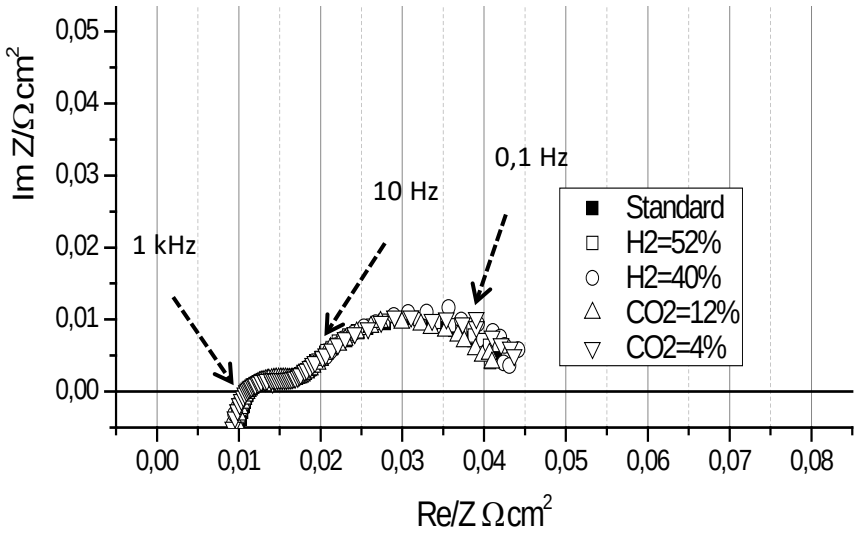

Figure 4: a,b,c: EIS spectra with 4 ppm of SO_2 in the cathodic stream @650 °C (a), 620 °C (b) and 680°C (c) (Standard composition: H2= 64% ; CO2= 6%). In this case EIS spectra don't show any changes that can be imputed to the SO_2 poisoning.

As the EIS plots (fig. 4,a, b, c), the I-V curves (fig.5 a, b, c) clearly visualize the change in temperature, since the increase of electrolyte conductivity with temperature becomes apparent under current swap conditions. However, it is peculiar that the cell performance at higher temperature (680 °C) is not noticeably higher than at 650 °C, in the same way as the performance at lower temperature (620 °C) is significantly reduced. This may be due to reaction sluggishness or other ageing effects resulting from having operated the cell first (in chronological order) at lower temperatures, as we shall observe later as well. The behaviour in terms of voltage dependence on variation of the selected parameters is the same as recorded in the "clean" case (fig. 2).

a)

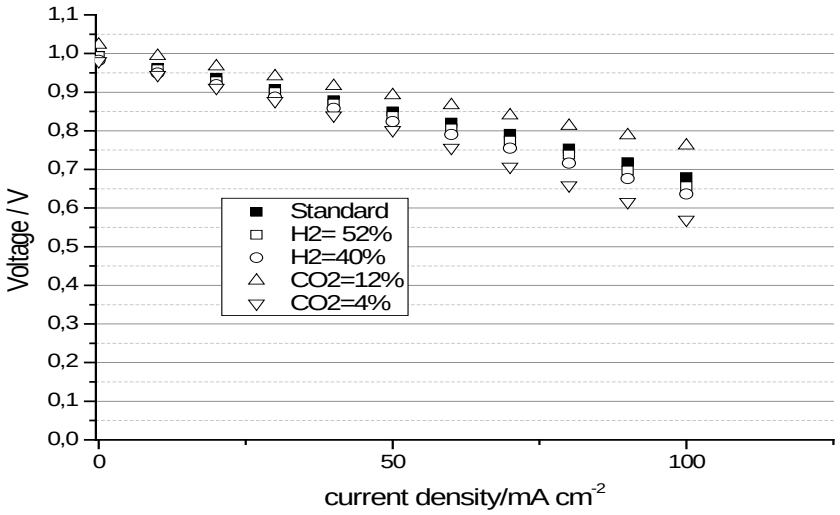

b)

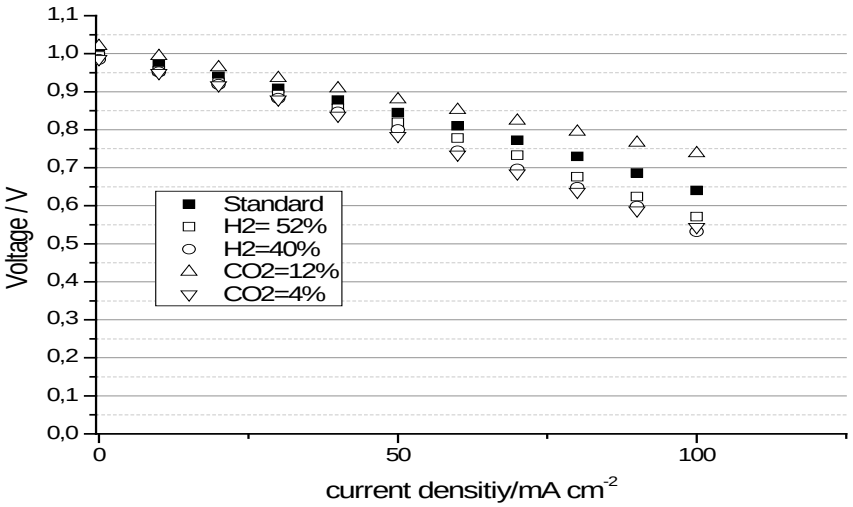

c)

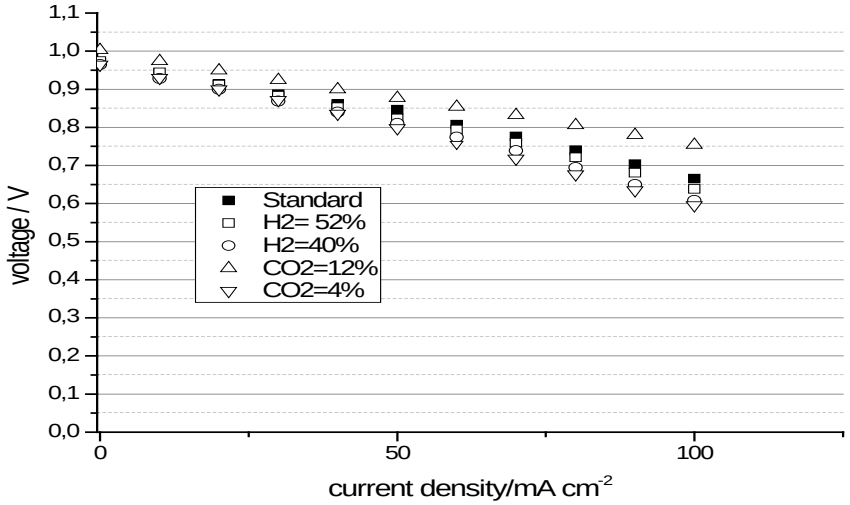

Figure 5 a,b,c: I-V curves with 4 ppm of SO_2 in the cathodic stream @ 650 °C (a), 620 °C (b), 680 °C (c)(Standard composition: H_2= 64% ; CO_2= 6%). The main differences noticeable between the figures a,b,c are caused by the variation of operating temperatures.

Thereafter, cell #2 was tested under medium poisoning conditions, i.e.8 ppm of SO_2 were introduced in the cathodic stream. After 36 hours, 2 ppm of H_2S were observed at the anode outlet and the reference composition was modified according to the tests campaign (H_2 and CO_2 variation) as already done for 4 ppm.

Results in this case show a different behaviour in the EIS spectra(fig.6) compared with tests in both clean and low poisoning (4 ppm SO_2) conditions, showing an increased internal resistance of the cell when the CO_2 molar fraction decreases compared to the standard gas composition. The reason of this behaviour has to be found in the reaction 3: when SO_2 is introduced in the cathode stream, it rapidly reacts with the electrolyte consuming CO_3^{2-} charge carriers, with a consequent decrease in the electrolyte conductivity revealed by the increasing of ohmic resistance. This behaviour is more evident when the CO_2 molar fraction decreases because of the shorter supply of fresh CO_3^{2-} ions, so that the cathodic reaction is less favoured.

Results at 650 °C are more explicative in this case because directly comparable with reference conditions. Moreover, the shift of the internal resistance is not caused by the temperature because all the spectra were obtained at 650 °C, allowing an immediate comparison with clean conditions (fig 3) when the shift of internal resistance wasn't noticeable.

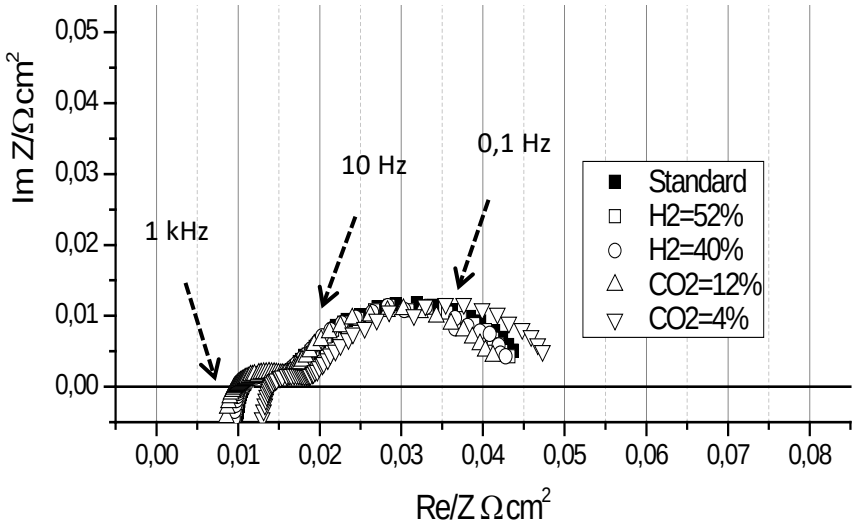

Figure 6: EIS spectra with 8 ppm of SO_2 introduced at cathode side @650 °C. IR resistance increase of 40% compared with standard 8ppm (H_2= 64%; CO_2= 6%) when CO_2 molar fraction decreases to 4%

Concerning the tests carried out with medium/high and high content of pollution, single cells (specimens #3 and #2) were operated with cathodic compositions at 16 ppm and 24 ppm SO_2. Introducing16 ppm of SO_2 at the cathode side of virgin MCFC #3,after 6 hours in pollution regime, 2.7 ppm of H_2S were detected at the anodic outlet via colorimetric syringe. This highlights the acceleration of the MCFC poisoning process with respect to the previous cases. The collection of IV curves measured varying the anodic and cathodic mixtures is shown in figure

7a (working temperature T= 650 °C), 7b (T= 620 °C) and 7c (T= 680 °C). Generally, the sulphur impact is reflected in the evident global performance decrease and the increase in IV curves spread. The latter is amplified at lower temperature (fig. 7b). It is underscored again that the graphs are presented in the same order as the test sequence: as before and, against theoretical prediction, a low performance at 680 °C is measured. As well as probable cumulated degradation effects due to sulphur poisoning, it is apparent that the tested cell suffers from previous operation at low temperature (620 °C), which inhibits the expected positive effect of higher temperature on MCFC performance. The marked variation of the cell I-V response over time would then suggests a rapid degradation, possibly due to a combination of the SO_2 level and the dynamics of the test conditions.

a)

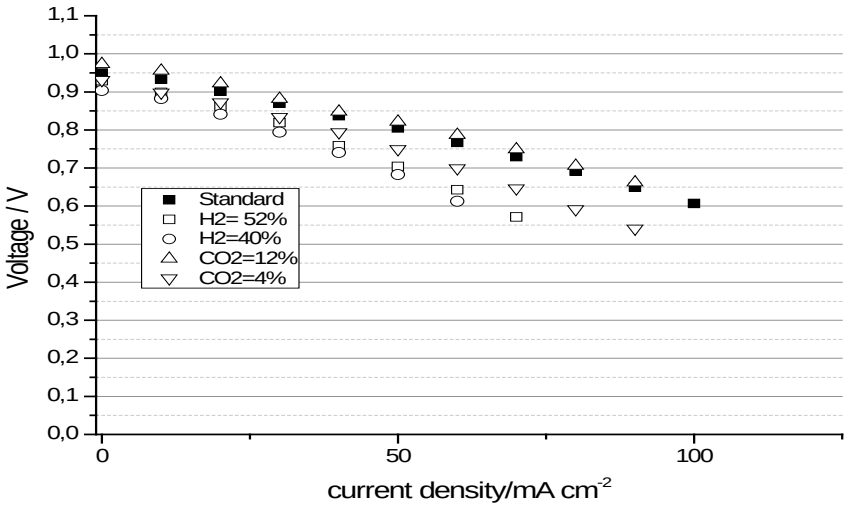

b)

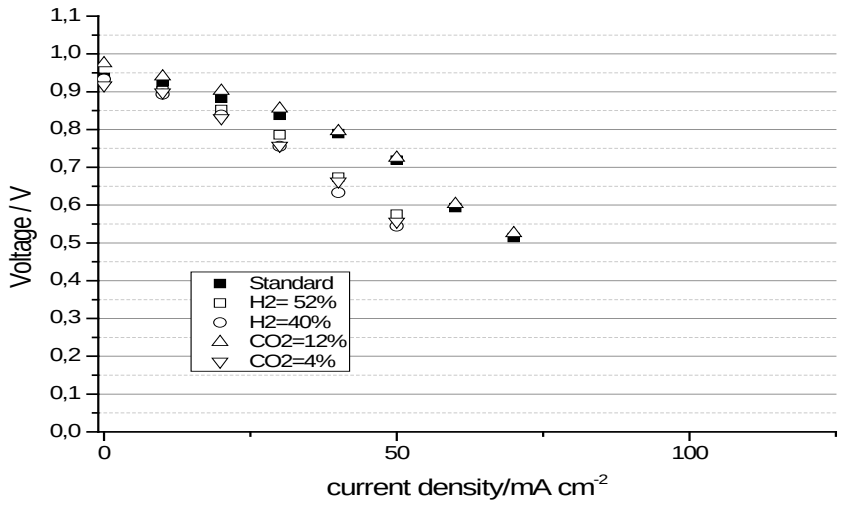

c)

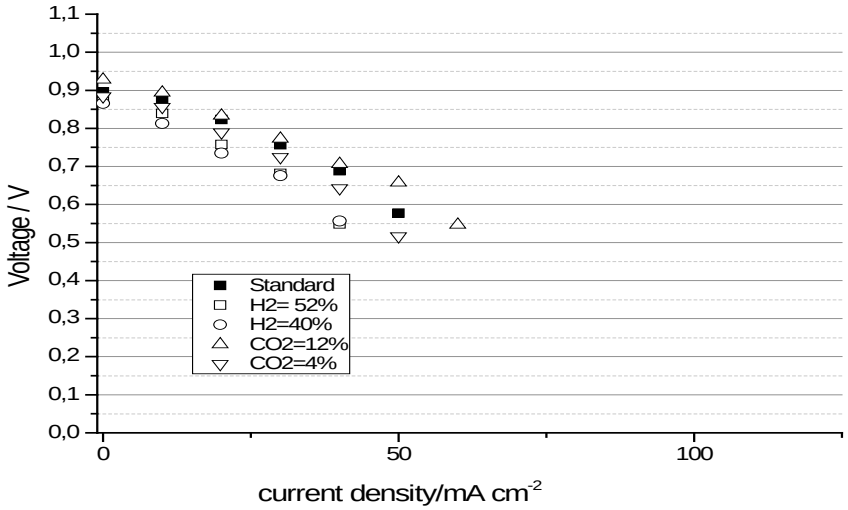

Figure 7a,b,c: I-V curves with 16 ppm of SO_2 in the cathodic stream @650 °C (a), 620 °C (b), 680 °C (c) (Standard composition: H_2= 64% ; CO_2= 6%).

Qualitative similar effects were finally obtained as results of tests at 24 ppm in terms of performance dependence on operating parameters, in spite of the different benches used for the tests execution. A H_2S concentration of 40 ppm was measured at the anode outlet. It is to be noted that during the experimental campaign no sulphur compounds were detected at any time at the cathode outlet. It is therefore deduced that all SO_2 entering the cathode chamber, immediately and completely reacts with the electrolyte (according to reaction 3), where subsequent reactions determine the fate of the sulphur introduced (reverse of reaction 4). The significant difference, in the amount of H_2S expelled from the anode in the two poisoning conditions tested on cell #2 (about 4 ppm and 40 ppm H_2S with 8 ppm and 24 ppm SO_2 respectively in the cathode mixture), may well be related to the accumulation of sulphate ions in the electrolyte during the first experiment when the same single cell was poisoned with 8ppm of SO_2 (table 2). The accumulation was clearly viewable, after the tests at 24ppm SO_2, when the cell was returned to clean conditions and H_2S continued to exit the anode for a further week of operation under load. These data serve to underline the importance of the dynamic component of the poisoning effects. The higher poisoning effect is evident also from the polarisation curves of Fig. 8a, b and c.

a)

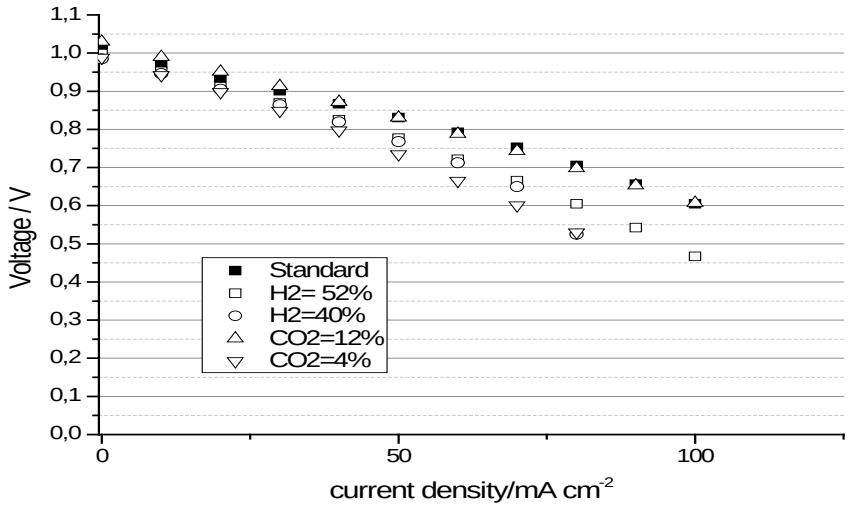

b)

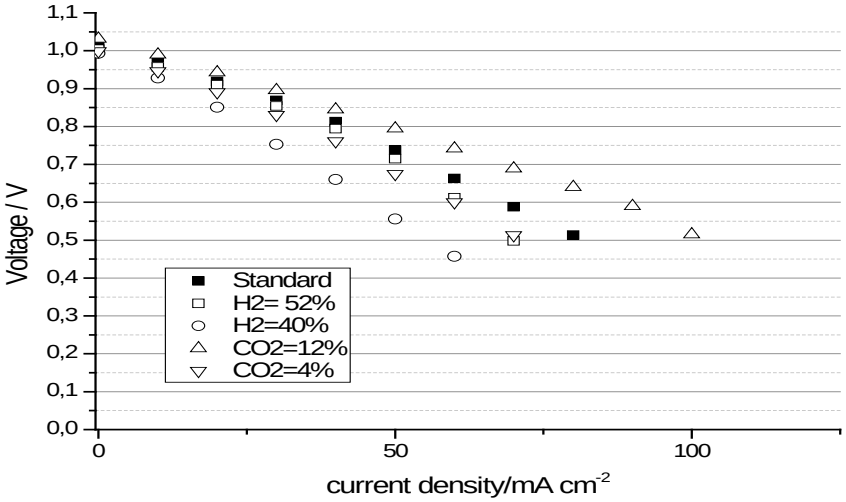

c)

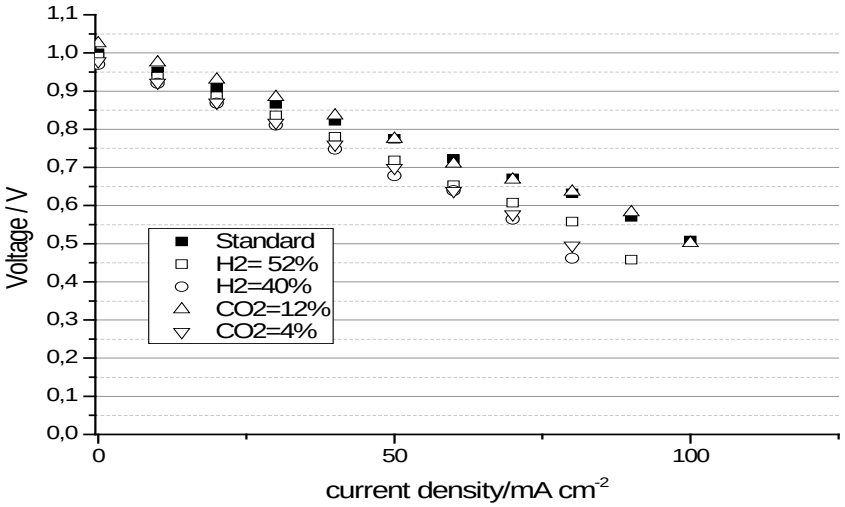

Figure 8a,b,c: I-V curves with 24 ppm of SO_2 in the cathodic stream @650 °C (a), 620 °C (b), 680 °C (c) (Standard composition: H_2= 64%; CO_2= 6%).

EIS spectra (figure 9a), instead, show an increase in the second semicircle, commonly associated to the mass transfer resistance. At the anode side, the increase in this resistance probably occurs because of the reduction of the number of active sites for hydrogen oxidation. Moreover, the effects of the increase in mass transfer resistance are more evident for low contents of hydrogen. This trend is confirmed by the EIS spectra carried out at 620 °C and 680 °C (fig. 9b-9c).Additionally, it is clear that the anode-side (hydrogen-side) poisoning effects are more significant at lower operating temperature, confirming previous observations regarding H_2S fed to the anode side [20].

a)

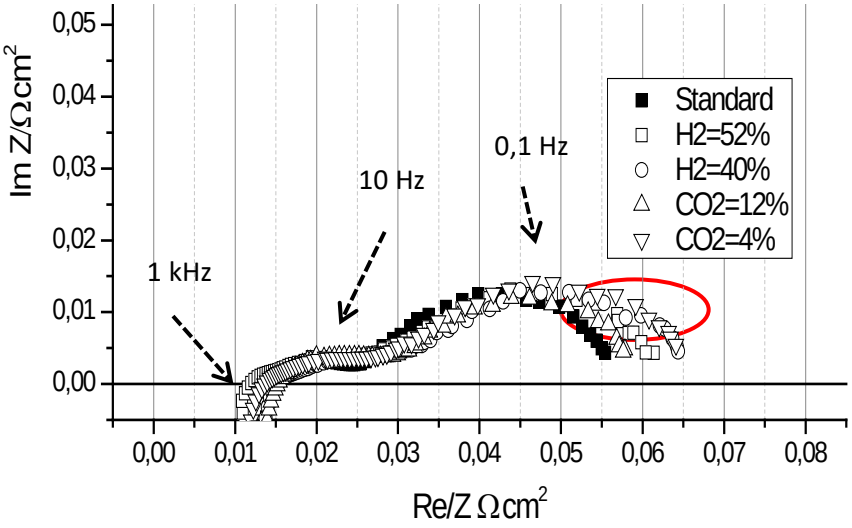

b)

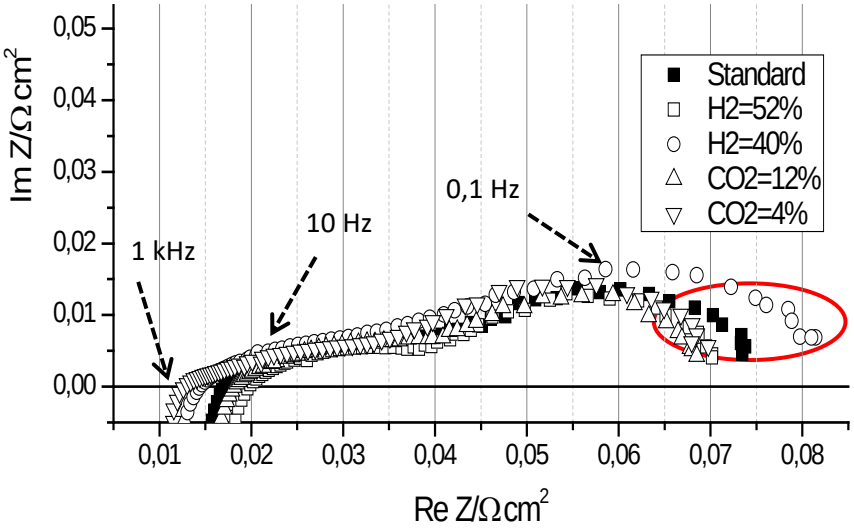

c)

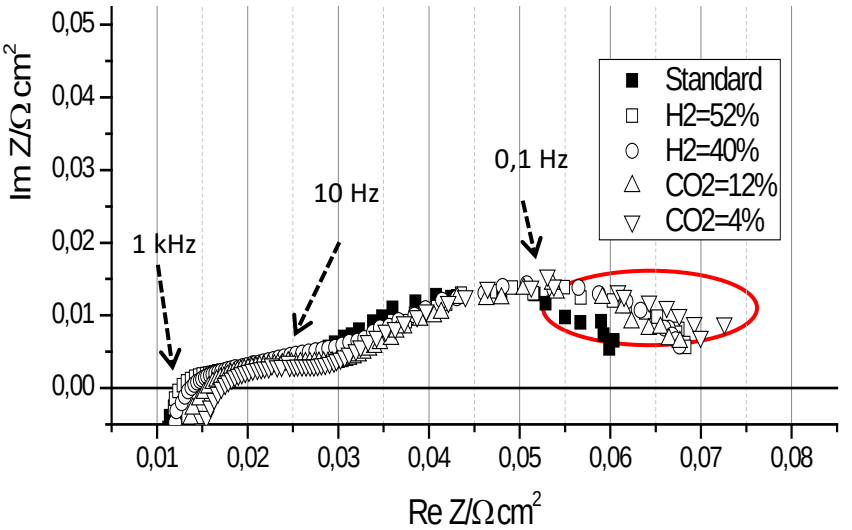

Figure 9: a,b,c: EIS spectra with 24 ppm of SO_2 in the cathodic stream @650 °C (a), 620 °C (b) and 680°C (c) (Standard composition: H2= 64%; CO2= 6%)

The combination of multiple effects, due to the injection of sulphur dioxide with different concentrations at the cathode, is more evident comparing the EIS spectra (figure 10) acquired on cell #2 under the three relevant phases of the experiment campaign: pre-poisoning, post- 8 ppm poisoning (in absence of SO_2) and post- 24 ppm poisoning (in absence of SO_2), at reference operating conditions (as detailed in table 1). As already discussed, instead, in the case of 4ppm SO_2, same spectra were acquired during post-poisoning and pre-poisoning operation, implying that no relevant effects can be detected with such small amount of pollutant agent.

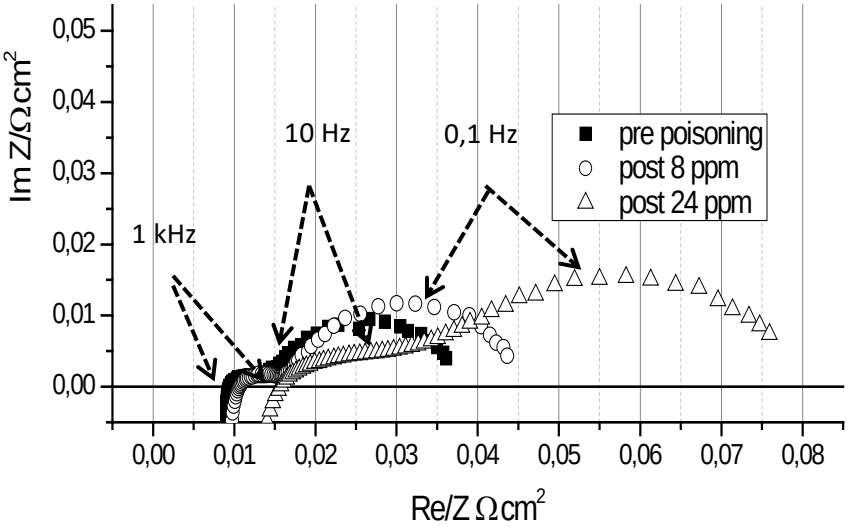

Figure 10: EIS spectra at standard conditions (no SO_2 fed to the cathode): before poisoning, after poisoning with 8 ppm and after poisoning with 24 ppm.

After tests with 24 ppm of SO_2, the cell was operated with clean gas in standard conditions to observe if an eventual performance recovery could be observed: the anode continued to expel H_2S for over a week, without any sulphur dioxide fed at the cathode. The degradation of the cell was too advanced to see any benefit in terms of performance (IV and EIS curves). As already remarked, this indicates that a significant accumulation of sulphur took place inside the cell, subsequently released once the cell was operated in clean conditions.

Post mortem analysis

After operation, cell specimens were dismantled and disassembled, to separate the components forming the single cell. Aiming to highlight differences in poisoning according to specific testing conditions, a further test was scheduled with respect to the campaign described in Section 3.

In particular, to have a comparative case-analysis relative to long-term low poisoning conditions, the virgin cell #4 was tested under reference conditions (bold values in Table 1), except for SO_2 content and test duration (1ppm SO_2; 1,000 h). No regeneration was performed.

Regarding tests scheduled in Section 3, instead, cell specimen #3, exposed to medium/high poisoning for a short time (16 ppm SO_2; 230h), it was chosen to perform EDX analysis because of the significant degradation effect discussed above and the absence of a subsequent regeneration phase.

Post mortem analysis was therefore performed on cell specimens #3 and #4. It is remarked that details (specifically concerning quantitative analysis) cannot be presented due to confidentiality agreements with the cell supplier.

Regarding cell #4, the following evidence (fig. 11) was provided by EDX analysis:

- The MCFC specimen does not show sulphur presence on cathode and electrolyte.

- The sulphur is identified on the anode with two components: a weak isotropic one (0.1-0.4% weight fraction) and the second, localized as drop-like accumulations (smooth and oval deposits, distinct from the background).
- Sulphur is identified alongside the potassium (but not the contrary) and complementary to the nickel as clearly evident from the K and S EDX maps in fig. 11.
- The punctual analysis on a restricted area, characterized by sulphur drop-like accumulations, shows elements (K, S, O) concentrations compatible with K_2SO_4 formation.

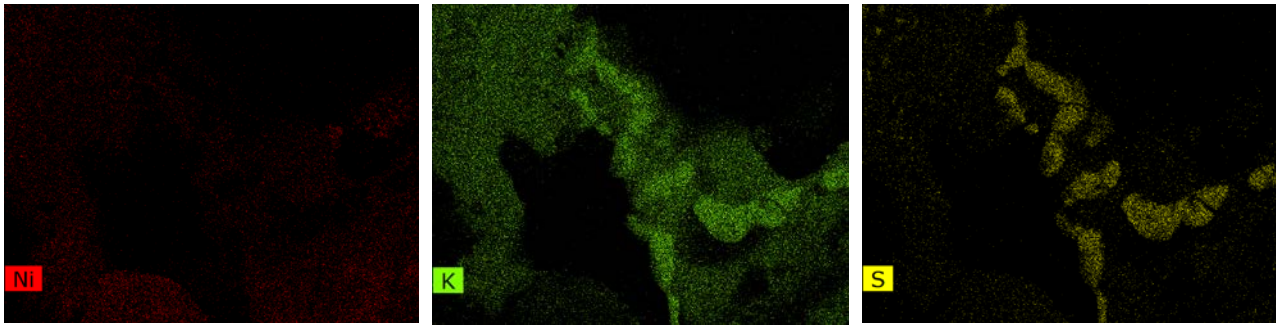

Figure 11. Anode detail of MCFC after 1.000 hours under 1 ppm of SO_2.

In the case of 230 hours operation under 16 ppm of SO_2, instead, the EDX analysis of the MCFC specimen #3 gave the following outcomes (fig. 12, 13, 14):

- The MCFC presents an increasing sulphur concentration from the cathode (0.15-0.25% weight fraction), to the electrolyte (0.3% at the cathode side and 0.45% at the anode side, always expressed as weight fractions) and finally to the anode, where the concentration increases suddenly (3%) on the electrolyte interface.
- At the cathode, sulphur has a weak and almost uniform distribution (S EDX map of fig. 12) as compared to the potassium-like distribution (K EDX map of fig. 12); in particular, there is no correlation with the potassium gatherings (K-S EDX map of fig. 12).
- The sulphur gatherings (potassium sulphate, probably) begin to appear on the electrolyte (S EDX map of fig. 13).
- The high anodic sulphur concentration (S EDX map of fig. 14) does not show localized gatherings, since they seem to follow the electrolyte traces (in particular the potassium distribution, as evident from the comparison between K and S EDX maps) and to be complementary to the nickel distribution.
- By increasing the distance from the anode-electrolyte interface, sulphur and potassium become residual (S<0.1% weight fraction).

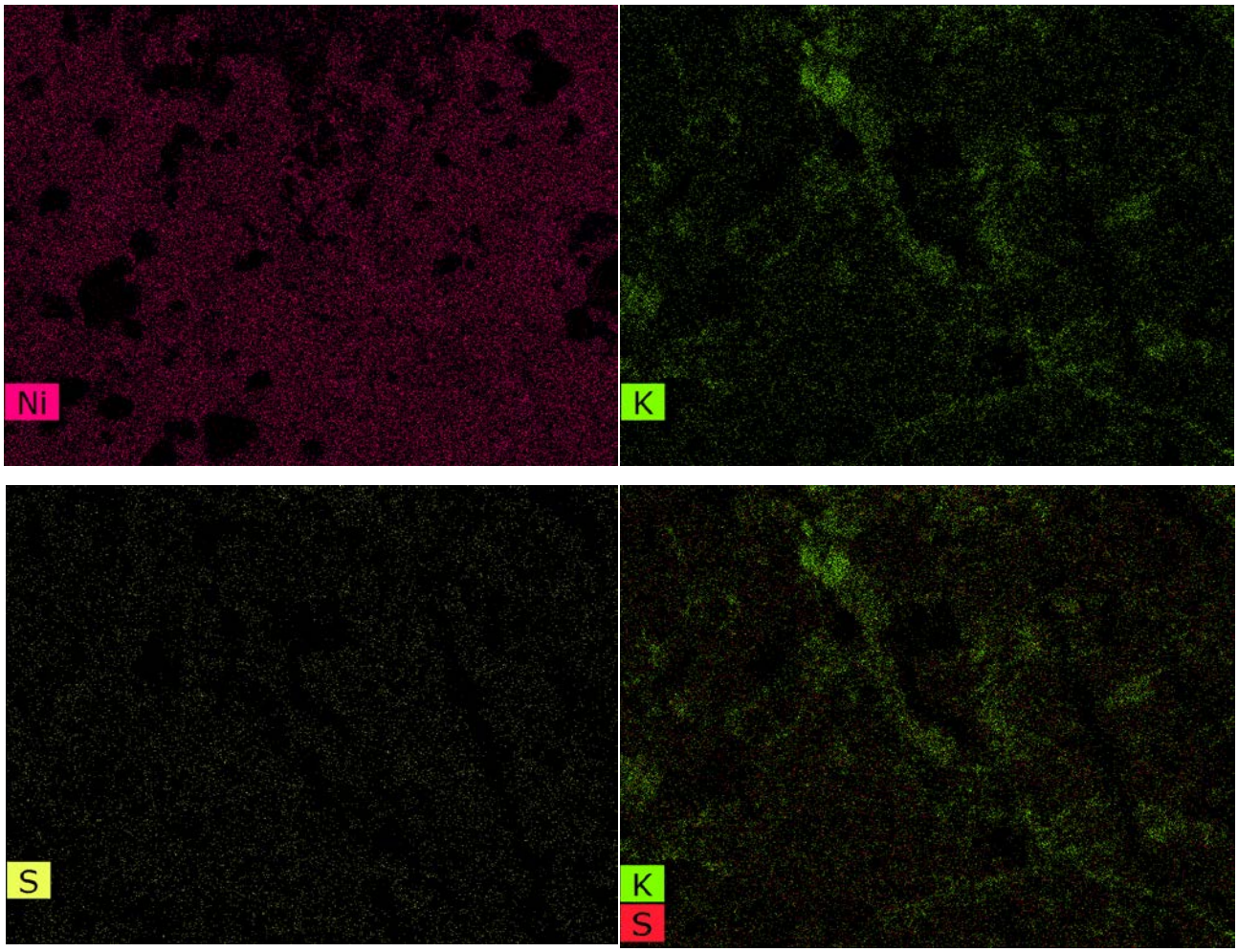

Figure 12. Cathode detail of MCFC after 230 hours under 16 ppm of SO_2.

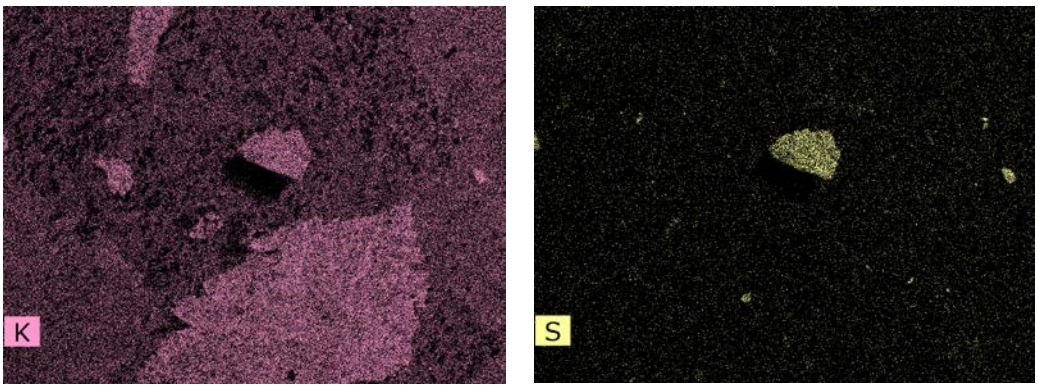

Figure 13. Electrolyte detail of MCFC after 230 hours under 16 ppm of SO_2.

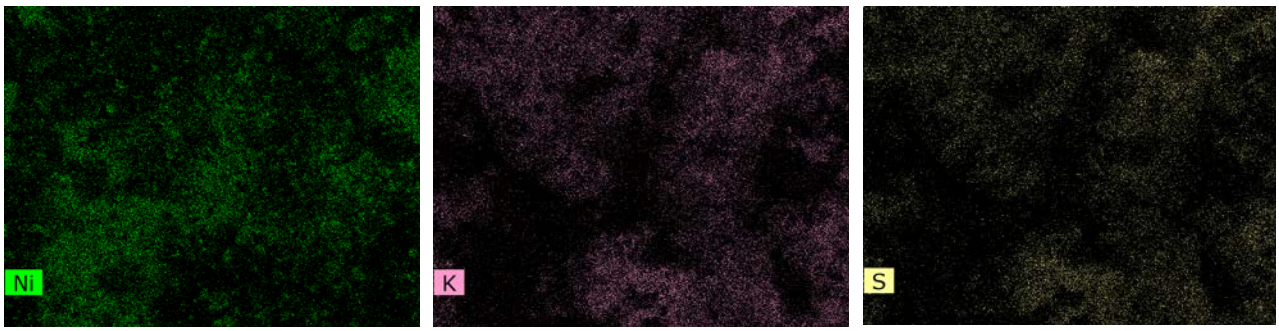

Figure 14. Anode detail of MCFC after 230 hours under 16 ppm of SO_2.

It is moreover remarked that EDX analysis is not sensible to lithium, which would have an expected distribution similar to that for potassium. Moreover, it is seems that in the case of a MCFC specimen exposed for long-term to low SO_2 poisoning (fed at the cathode), the sulphur accumulates in an appreciable way only at the anode side (in drop-like shapes), while under higher SO_2 content (even if for a shorter period) it produces a more uniform and spread-out distribution.

5. Conclusions

The experimental campaign carried out in this work puts in evidence the strict correlation between MCFC operating parameters and sulphur dioxide concentration introduced at the cathode side.

The primary effect of poisoning (loss of ionic transfer in the electrolyte) was more evident during the set of experiments at 8 ppm of SO_2 added in the cathode feeding mixture. Moreover, the variation of operating parameters highlighted an increased ohmic resistance when the CO_2 content was 4% underlining the effect of usurpation of charge carriers by sulphur ions determining a lower conductivity of the electrolyte. The secondary effect (release of H_2S at the anode side with associated poisoning of electro-catalytic sites) started to contribute to the performance decay when a higher concentration of SO_2 was used (24 ppm); the EIS spectra, in fact, showed a significant change of mass transfer resistance. Also in this case the variation of experimental parameters (particularly H_2) gave important information about the poisoning mechanism.

Post mortem analysis, performed on a cell exposed to medium/high sulphur poisoning (cell #3), showed a high selectivity of elemental sulphur with potassium. This was more evident in the samples of the interface between anode and electrolyte. Furthermore, EDX analysis evidenced an accumulation of sulphur at anode side, probably in the form of potassium sulphate, evolved during the operation of the cell. This assumption is confirmed by the fact that, in case of specimen #2, H_2S continued to flow out from the anode for one week, once that the poisoning (24 ppm) was interrupted.

The results obtained in this work give new inputs to better understand the complex degradation mechanism caused by sulphur dioxide feeding at the cathode. Nevertheless, a new test campaign is expected next to lead a deeper quantitative analysis by isolating the poisoning effects from pre-experimental condition.

Acknowledgements

The work was partly supported by H2FC European Infrastructure Project (Integrating European Infrastructure to support science and development of Hydrogen and Fuel Cell Technologies towards European Strategy for Sustain- able Competitive and Secure Energy) Theme [INFRA-2011-1.1.16.], Grant agreement 284522.

References

[1] K. Sugiura, K. Takei, K. Tanimoto, and Y. Miyazaki, “The carbon dioxide concentrator by using MCFC,” *J. Power Sources*, vol. 118, no. 1–2, pp. 218–227, May 2003.

[2] G. Discepoli, G. Cinti, U. Desideri, D. Penchini, and S. Proietti, “Carbon capture with molten carbonate fuel cells: Experimental tests and fuel cell performance assessment,” *Int. J. Greenh. Gas Control*, vol. 9, pp. 372–384, Jul. 2012.

[3] G. Discepoli, J. Milewski, and U. Desideri, “Off-design operation of coal power plant integrated with natural gas fueled molten carbonate fuel cell as CO2 reducer,” *Int. J. Hydrogen Energy*, pp. 1–11, Feb. 2016.

[4] I. Rexed, M. Della Pietra, S. J. McPhail, G. Lindbergh, and C. Lagergren, “Molten carbonate fuel cells for CO2 separation and segregation by retrofitting existing plants – An analysis of feasible operating windows and first experimental findings,” *Int. J. Greenh. Gas Control*, vol. 35, pp. 120–130, Apr. 2015.

[5] J. Milewski, J. Lewandowski, and A. Miller, “Reducing CO2 emissions from a coal fired power plant by using a molten carbonate fuel cell,” *Chem. Process Eng.*, vol. 30, no. 2, pp. 341–350, 2009.

[6] D. Sánchez, S. Ubertini, J. M. Muñoz de Escalona, and R. Chacartegui, “Potential of molten carbonate fuel cells to reduce the carbon footprint of large reciprocating engines,” *Int. J. Hydrogen Energy*, vol. 39, no. 8, pp. 4081–4088, Mar. 2014.

[7] U. Desideri, S. Proietti, P. Sdringola, G. Cinti, and F. Curbis, “MCFC-based CO2 capture system for small scale CHP plants,” *Int. J. Hydrogen Energy*, vol. 37, no. 24, pp. 19295–19303, Dec. 2012.

[8] J. Milewski, W. Bujalski, M. Wołowicz, K. Futyma, J. Kucowski, and R. Bernat, “Experimental investigation of CO2 separation from lignite flue gases by 100 cm2 single Molten Carbonate Fuel Cell,” *Int. J. Hydrogen Energy*, vol. 39, no. 3, pp. 1558–1563, Jan. 2014.

[9] S. Campanari, “Carbon dioxide separation from high temperature fuel cell power plants,” *J. Power Sources*, vol. 112, no. 1, pp. 273–289, Oct. 2002.

[10] S. Campanari, P. Chiesa, and G. Manzolini, “CO2 capture from combined cycles integrated with Molten Carbonate Fuel Cells,” *Int. J. Greenh. Gas Control*, vol. 4, no. 3, pp. 441–451, May 2010.

[11] P. Chiesa, S. Campanari, and G. Manzolini, “CO2 cryogenic separation from combined cycles integrated with molten carbonate fuel cells,” *Int. J. Hydrogen Energy*, vol. 36, no. 16, pp. 10355–10365, Aug. 2011.

[12] P. Greppi, B. Bosio, and E. Arato, “Membranes and Molten Carbonate Fuel Cells to Capture CO 2 and Increase Energy Production in Natural Gas Power Plants,” *Ind. Eng. Chem. Res.*, vol. 52, no. 26, pp. 8755–8764, 2013.

[13] J. Milewski, G. Discepoli, and U. Desideri, “Modeling the performance of MCFC for various fuel and oxidant compositions,” *Int. J. Hydrogen Energy*, vol. 39, no. 22, pp. 11713–11721, Jul. 2014.

[14] I. Rexed, C. Lagergren, and G. Lindbergh, “Effect of sulfur contaminants on MCFC performance,” *Int. J. Hydrogen Energy*, vol. 39, no. 23, pp. 12242–12250, Aug. 2014.

[15] N. Di Giulio, B. Bosio, J. Han, and S. J. McPhail, “Experimental analysis of SO2 effects on Molten Carbonate Fuel Cells,” *Int. J. Hydrogen Energy*, vol. 39, no. 23, pp. 12300–12308, Aug. 2014.

[16] N. Di Giulio, E. Audasso, B. Bosio, J. Han, and S. J. McPhail, “Experimental influence of operating variables on the performances of MCFCs under SO2 poisoning,” *Int. J. Hydrogen Energy*, vol. 40, no. 19, pp. 6430–6439, 2015.

[17] D. Weaver and J. Winnick, “Sulfation of the molten carbonate fuel cell anode,” *J. Electrochem. Soc.*, vol. 136, no. 6, 1989.

[18] V. Cigolotti, S. J. McPhail, A. Moreno, S. P. Yoon, J. H. Han, S. W. Nam, and T.-H. Lim, “MCFC fed with biogas: Experimental investigation of sulphur poisoning using impedance spectroscopy,” *Int. J. Hydrogen Energy*, vol. 36, no. 16, pp. 10311–10318, Aug. 2011.

[19] H. Devianto, E. Simonetti, S. J. McPhail, F. Zaza, V. Cigolotti, C. Paoletti, A. Moreno, A. La Barbera, and I. Luisetto, “Electrochemical impedance study of the poisoning behaviour of Ni-based anodes at low concentrations of H2S in an MCFC,” *Int. J. Hydrogen Energy*, pp. 1–7, Apr. 2012.

[20] N. Di Giulio, B. Bosio, V. Cigolotti, and S. W. W. Nam, “Experimental and theoretical analysis of H2S effects on MCFCs,” *Int. J. Hydrogen Energy*, vol. 37, no. 24, pp. 19329–19336, Dec. 2012.

[21] F. Zaza, C. Paoletti, R. Lo Presti, E. Simonetti, and M. Pasquali, “Studies on sulfur poisoning and development of advanced anodic materials for waste-to-energy fuel cells applications,” *J. Power Sources*, vol. 195, no. 13, pp. 4043–4050, Jul. 2010.

[22] F. Zaza, C. Paoletti, R. LoPresti, E. Simonetti, and M. Pasquali, “Multiple regression analysis of hydrogen sulphide poisoning in molten carbonate fuel cells used for waste-to-energy conversions,” *Int. J. Hydrogen Energy*, vol. 36, no. 13, pp. 8119–8125, Jul. 2011.

[23] E. Sisani, G. Cinti, G. Discepoli, D. Penchini, U. Desideri, and F. Marmottini, “Adsorptive removal of H2S in biogas conditions for high temperature fuel cell systems,” *Int. J. Hydrogen Energy*, vol. 39, no. 36, pp. 21753–21766, Dec. 2014.

[24] B. Bosio, N. Di Giulio, S. W. Nam, and A. Moreno, “An effective semi-empiric model for MCFC kinetics: Theoretical development and experimental parameters identification,” *Int. J. Hydrogen Energy*, vol. 39, no. 23, pp. 12273–12284, Aug. 2014.